Phytopathology Research

RESEARCH

Open Access

XrvB regulates the type III secretion system by directly repressing *hrpG* transcription in *Xanthomonas oryzae* pv. *oryzicola*

Jian-Ling Peng[1†], Jia-Feng Shi[1†], Zeng-Feng Ma[2], Xiao-Long Zhou[2], Wen-Xin Ye[1], Qian Su[1], Gui-Ning Zhu[3], Ji-Liang Tang[1], Rui-Fang Li[3*] and Guang-Tao Lu[1*]

Abstract

Xrv proteins are a group of regulators in *Xanthomonas* spp., belonging to the histone-like nucleoid-structuring (H-NS) proteins of Gram-negative bacteria. The rice bacterial leaf streak pathogen *Xanthomonas oryzae* pv. *oryzicola* (*Xoc*) harbors three Xrv proteins, the XrvA, XrvB, and XrvC. Here, we report that in *Xoc*, the XrvB but not XrvA and XrvC is involved in negative regulation of the type III secretion system (T3SS) encoded by *hrp* genes. As with other *Xanthomonas* spp., the T3SS is an essential virulence determinant of *Xoc* and the expression of the *hrp* genes in *Xoc* is controlled by the HrpG/HrpX regulatory cascade. HrpG positively regulates the expression of HrpX, which in turn activates the transcription of the *hrp* genes. We provide evidences to demonstrate that the XrvB binds to the promoter region of *hrpG* and represses its transcription. Furthermore, we found that XrvB production was induced in the *Xoc* cells cultured in a nutrient-rich medium compared to a *hrp*-inducing minimal medium. We also found that in *Xoc*, the *hrpG* expression level is inversely correlated with the content of XrvB, and XrvB occupancy at *hrpG* promoter region is positively correlated with XrvB levels. Our data suggest that XrvB is a determinative factor controlling the expression levels of HrpG. In addition, mutation analysis revealed that the *Xoc* XrvB also plays positive roles in regulating bacterial growth, cell motility, and stress tolerance. Our findings provide important insights into the molecular mechanism of T3SS expression regulation in *Xoc*.

Keywords *Xanthomonas oryzae*, T3SS, *hrp* genes, H-NS protein, Xrv protein

Introduction

The Gram-negative bacterial species *Xanthomonas oryzae* comprises two pathovars that are able to infect rice, the *Xanthomonas oryzae* pv. *oryzae* (*Xoo*) and *Xanthomonas oryzae* pv. *oryzicola* (*Xoc*). The former causes bacterial leaf blight, while the later causes bacterial leaf streak. Both are the major rice diseases and the pathogens can serve as models for studying molecular interactions between phytopathogenic bacteria and monocot plants (Niño-Liu et al. 2006; Mansfield et al. 2012; Zhang and Wang 2013; Long et al. 2018). As with many other bacterial pathogens, the type III secretion system (T3SS) that encoded by a cluster of over 20 hypersensitive response and pathogenicity (*hrp*) genes is an essential

†Jian-Ling Peng and Jia-Feng Shi have contributed equally to this work.

*Correspondence:
Rui-Fang Li
ruifangli@gxaas.net
Guang-Tao Lu
lugt@gxu.edu.cn
[1] State Key Laboratory for Conservation and Utilization of Subtropical Agro-Bioresources, College of Life Science and Technology, Guangxi University, Nanning 530004, China
[2] Rice Research Institute, Guangxi Academy of Agricultural Sciences, Nanning 530007, China
[3] Guangxi Key Laboratory of Biology for Crop Diseases and Insect Pests, Plant Protection Research Institute, Guangxi Academy of Agricultural Sciences, Nanning 530007, China

virulence determinant of *X. oryzae* (Zou et al. 2006; Niu et al. 2022). Mutation in *Xoc* or *Xoo hrp* genes abolished the secretion of a range of effector proteins, resulting in reduced pathogenicity on the host plant rice and loss of ability to trigger hypersensitive reaction (HR) in the nonhost plant *Nicotiana benthamiana* (Zou et al. 2006). It is clear that similar to other *Xanthomonas* spp., the expression of the *hrp* genes (as well as most of the genes encoding the effector proteins) is induced in plant tissues and minimal media, and is directly activated by the AraC family transcriptional regulator HrpX in *X. oryzae*. Notably, the transcription of *hrpX* gene is positively modulated by the OmpR family regulator HrpG (Teper et al. 2021).

Xrv (*Xanthomonas* regulator of virulence) proteins are members of histone-like nucleoid-structuring (H-NS) proteins (Feng et al. 2009; Kametani-Ikawa et al. 2011; Liu et al. 2016), which are a class of abundant small DNA-binding proteins and are widespread in Gram-negative bacteria. Besides playing a role in genome evolution and DNA condensation, members of the H-NS protein family can act as negative transcriptional regulators to regulate many important cellular processes and pathogenesis (Tendeng and Bertin 2003; Dorman 2004; Qin et al. 2019). Previous studies showed that *Xoo* encodes three Xrv proteins (XrvA, XrvB, and XrvC), where they play a role in full virulence with divergent impacts on T3SS expression in different strains (Feng et al. 2009; Kametani-Ikawa et al. 2011; Liu et al. 2016). The XrvA in the Chinese *Xoo* strain 13,751 plays a positive role in virulence, HR, the production of extracellular polysaccharide (EPS), and diffusible signal factor (DSF), and is a negative regulator in intracellular glycogen accumulation (Feng et al. 2009). The XrvB in the Japanese *Xoo* strain MAFF311018 is a virulence protein but negatively regulates *hrp* gene expression (Kametani-Ikawa et al. 2011). However, the XrvC in the Philippines *Xoo* strain PXO99^{A} is involved in positive regulation of *hrp* gene expression (Liu et al. 2016).

Despite the above-mentioned advances for Xrv proteins in *Xoo*, little is known for the function of the Xrv proteins in *Xoc*. Similar to *Xoo*, the Chinese *Xoc* strain GX01 harbors three Xrv proteins (Niu et al. 2022). In this work, we investigated the role of these proteins in HR induction. We found that XrvB but not XrvA and XrvC is involved in the HR induction on the nonhost plant *Nicotiana benthamiana*. Here, we provide evidences to demonstrate that *Xoc* XrvB directly binds to *hrpG* promoter to repress its transcription, thereby affecting T3SS expression. Furthermore, the *Xoc* XrvB is involved in positive regulation of bacterial growth, cell motility, and stress tolerance. Deletion of *xrvB* resulted in a significant reduction in the pathogenicity of *Xoc*.

Results

Xoc XrvB plays a negative role in HR induction

Genome analysis revealed that the *Xoc* strain GX01 has three ORFs encoding H-NS or H-NS-like proteins. They are XOCgx_0907, XOCgx_1228, and XOCgx_2828 (Accession numbers QEO95901.1, QEO96221.1, and QEO97817.1). The amino acid sequences of XOCgx_0907, XOCgx_1228, and XOCgx_2828 share high similarity (95.4%, 83.8%, and 97%) to that of the *Xoo* XrvB (strain MAFF311018) (Kametani-Ikawa et al. 2011), XrvC (strain PXO99^{A}) (Liu et al. 2016), and XrvA (strain 13,751) (Feng et al. 2009). Accordingly, we named the proteins that are encoded by *XOCgx_0907*, *XOCgx_1228*, and *XOCgx_2828* as XrvB, XrvC, and XrvA, respectively. The XrvA and XrvC are composed of 133 and 130 amino acids, respectively, which share 57.9% similarity (Additional file 1: Figure S1). The XrvB is a 153-amino-acid protein which shares 28.8% and 26.1% similarity with XrvA and XrvC, respectively (Additional file 1: Figure S1).

To explore the role of the *Xoc* Xrv proteins in T3SS, we constructed their deletion mutants (Δ*xrvA*, Δ*xrvB*, and Δ*xrvC*), complemented strains (CΔ*xrvA*, CΔ*xrvB*, and CΔ*xrvC*), and overexpression strains (GX01/pB*xrvA*, GX01/pB*xrvB*, and GX01/pB*xrvC*) (Additional file 2: Table S1). To test the ability of these mutant strains in inducing HR in nonhost plants, the bacterial cells of *Xoc* strains were infiltrated at a cell concentration of OD_{600} of 0.5 (approximately 5×10^{8} CFU/mL) into the leaves of *Nicotiana benthamiana* plants. Results revealed that all the deletion mutants, complemented strains, and overexpression strains except GX01/pB*xrvB* elicited similar HR symptoms to the wild type (Fig. 1a and Additional file 1: Figure S2). Interestingly, although GX01/pB*xrvB* produced obvious HR symptoms at 48 h post-infiltration (hpi), the HR symptoms were significantly weaker within 36 hpi when compared to the wild type (Fig. 1a), indicating that overexpressing XrvB in GX01 could weaken and delay HR induction. However, a control strain GX01/pBBad22K (Additional file 2: Table S1) induced similar HR symptoms to the wild type (Fig. 1a and Additional file 1: Figure S2). These results suggest that *Xoc* XrvB but not XrvA and XrvC plays a role in HR elicitation. The effect of *Xoc* XrvB on HR induction was further estimated using the electrolyte leakage assay. Here, leaf tissues within the infiltration areas were collected at 24, 36, and 48 hpi. The results showed that the *xrvB* deletion mutant strain Δ*xrvB*, complemented strain CΔ*xrvB*, and the control strain GX01/pBBad22K induced similar levels of electrolyte leakage to the wild type at all the three tested time-points (Fig. 1b). However, the *xrvB*-overexpressing strain GX01/pB*xrvB* elicited much lower levels of HR at all the tested time-points, compared to the

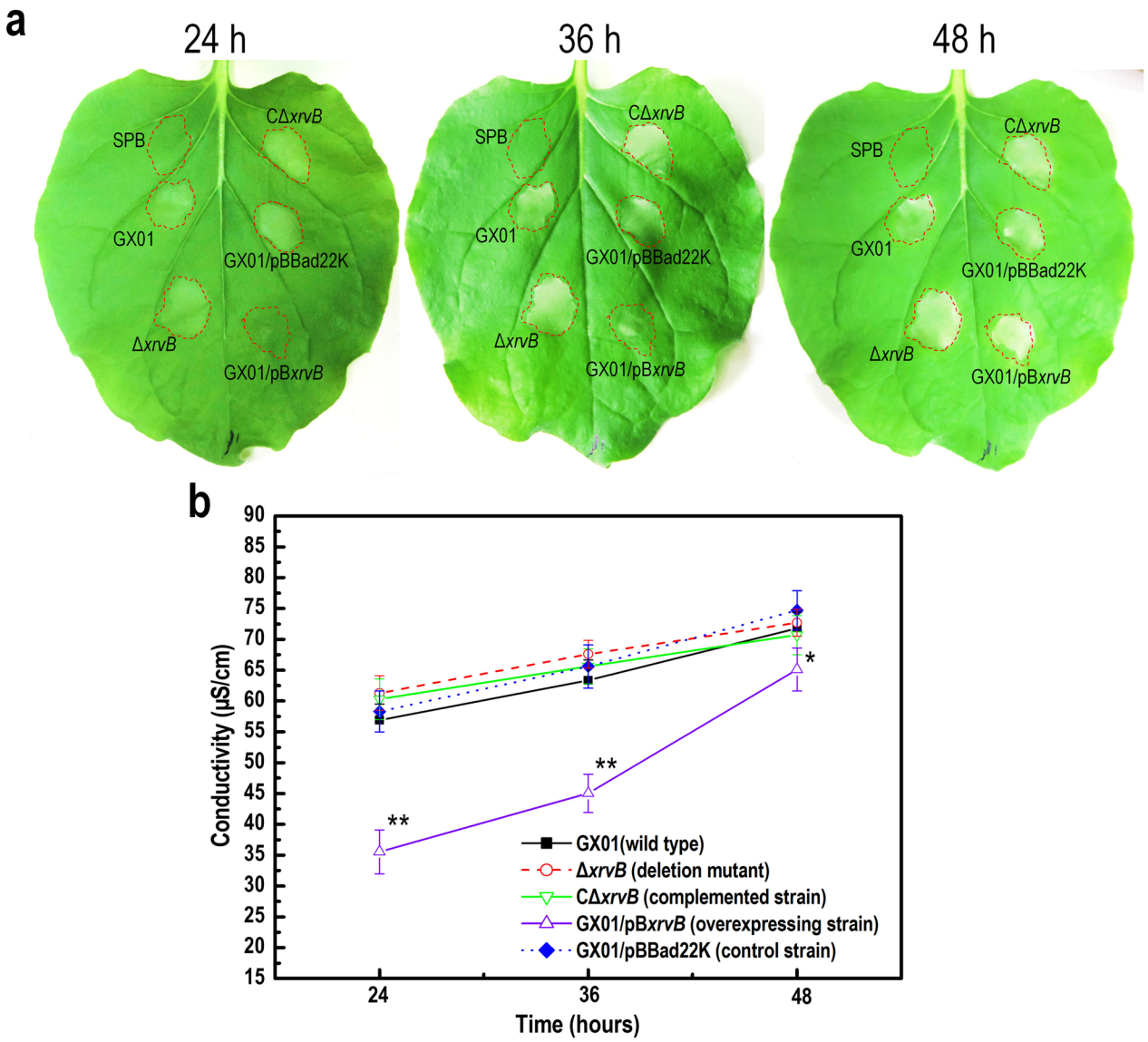

Fig. 1 XrvB is involved in HR induction in *Xoc*. Bacterial cells were cultured in NB medium and re-suspended in SPB to a concentration of OD_{600} at 0.5. The bacterial suspensions were infiltrated into the leaves of non-host plant *N. benthamiana*. **a** Hypersensitive response (HR) symptoms were observed at 24, 36, and 48 h post-infiltration (hpi). **b** Electrolyte leakage of *N. benthamiana* leaves infiltrated with *Xoc* strains were measured. For each sample, four 0.4 cm^2 leaf disks were collected from the bacteria-inoculated area and incubated in 5 mL ultrapure water. Conductivity was measured at 24, 36, and 48 hpi. The results presented are the mean ± SD (n = 3 biological replicates). *$P < 0.05$, **$P < 0.01$, significant difference from the wild-type strain, using Student's *t*-test

wild type. Taken together, the data indicate that *Xoc* XrvB suppresses HR elicitation.

Xoc XrvB negatively regulates T3SS gene expression

As mentioned above, the bacterial T3SS is responsible for HR induction. Because XrvB affects HR elicitation, it prompted us to estimate the function of XrvB on the expression of T3SS. To this end, we employed reverse transcription-quantitative real-time PCR (RT-qPCR) to analyze the transcription levels of a set of T3SS or T3SS-related genes in *Xoc xrvB* mutants (Δ*xrvB* and GX01/pB*xrvB*) and control strains (GX01 and GX01/pBBad22K). The tested genes include *hrpG* and *hrpX* which encode key regulators, and *hrpF*, *hrpB1*, *hrcV*, *hrcN*, and *hrcU* which encode T3SS apparatus proteins, and *xopL*, *xopR*, and *avrBs3* which encode the secreted effectors. The strains were cultured in the minimal medium XOM2 and the nutrient-rich medium NB,

respectively. RT-qPCR results demonstrated that the expression of all the tested genes was significantly up-regulated in the *xrvB* deletion mutant strain Δ*xrvB* compared to the wild-type GX01 in both media, but their expression was significantly down-regulated in the *xrvB*-overexpressing strain GX01/pB*xrvB* compared to the control strain GX01/pBBad22K (Fig. 2). This result suggests that *Xoc* XrvB plays a negative regulatory role in the transcription of T3SS genes in media. The XrvB-regulated expression of the T3SS genes was further determined by RT-qPCR during infection on rice plants. The result displayed that, similar to the observation in media, the transcription levels of all the tested genes were significantly up-regulated in Δ*xrvB* and were down-regulated in GX01/pB*xrvB* (Fig. 2). Therefore, XrvB also negatively regulates the transcription of T3SS genes in *Xoc* during infection.

We further examined the protein levels encoded by *hrpG* and *xopN* (another T3SS-secreted effector gene) using western blot assay. To achieve this, *Xoc* strains containing HrpG or XopN fused with the 3×Flag peptide tag in GX01 and the *xrvB* deletion mutant Δ*xrvB* were generated. The obtained strains were named GX01/HrpG::3×Flag, Δ*xrvB*/HrpG::3×Flag, GX01/XopN::3×Flag, and Δ*xrvB*/XopN::3×Flag (Additional file 2: Table S1). The strains were cultured in XOM2 and NB media, respectively, and their total proteins were extracted and analyzed by Western blotting. As shown in Fig. 3a, contents of the two tested proteins in the XrvB-deficient strain were higher than that in the wild-type strain, indicating that *Xoc* XrvB undermines HrpG and XopN production. The effect of overexpressing XrvB on HrpG and XopN production was also examined. To do this, the vector pBBad22K and the recombinant plasmid pB*xrvB* were introduced into the above strains, the resulting strains were named as GX01/HrpG::3×Flag/pBBad22K, GX01/HrpG::3×Flag/pB*xrvB*, GX01/XopN::3×Flag/pBBad22K, and GX01/XopN::3×Flag/pB*xrvB* (Additional file 2: Table S1), and the expressed proteins were used for western blotting assays. As shown in Fig. 3b, the protein levels of HrpG and XopN in the XrvB-overexpressing strains (i.e., the strains with pB*xrvB*) were much less compared to the wild-type strains (i.e., the strains with pBBad22K). These data

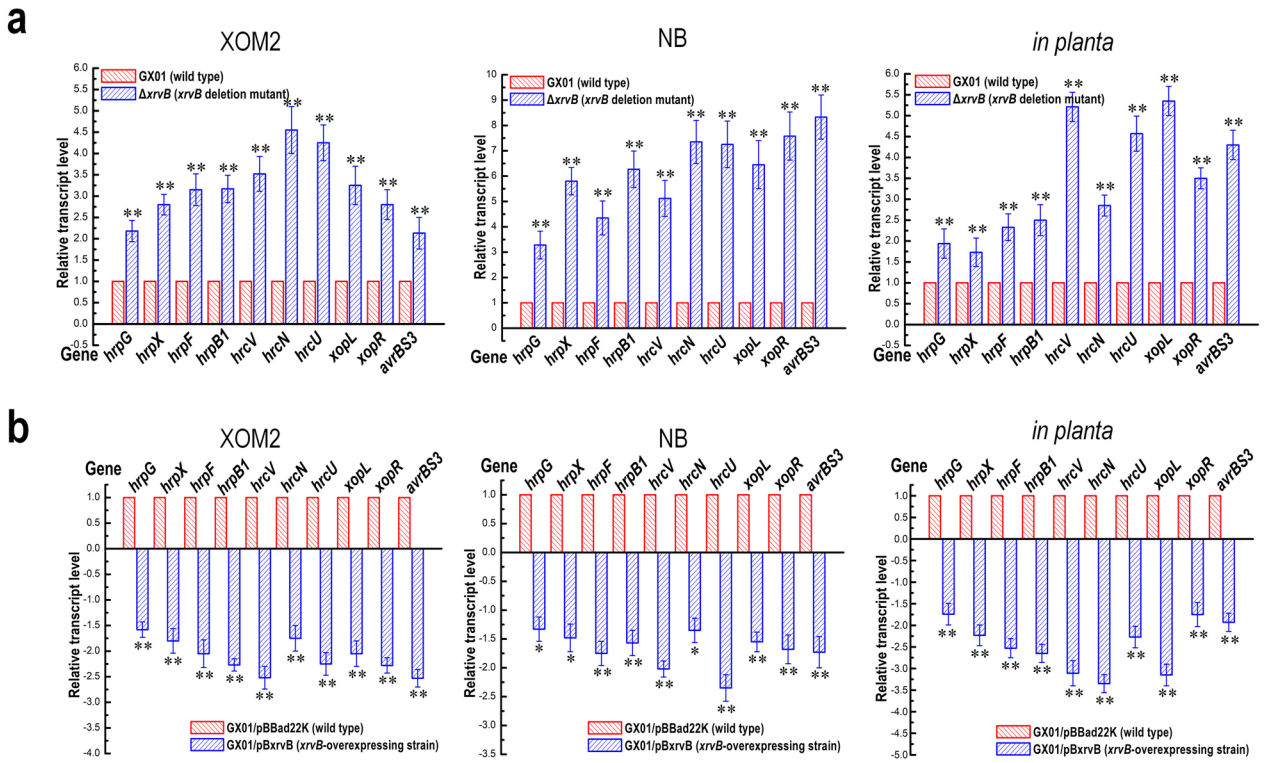

Fig. 2 Deletion or overexpression of XrvB in *Xoc* distinctly regulated the transcriptions of type III secretion system (T3SS) genes, revealed by RT-qPCR analysis. **a** Deletion of *xrvB* enhanced the transcription levels of T3SS genes. The *Xoc* wild-type strain GX01 and the *xrvB* deletion mutant Δ*xrvB* were cultured in XOM2 or NB to an OD_{600} of 0.6, or grown in host plants for 24 h, and total RNA was isolated. The expression levels of several *hrp/hrc* genes encoding the components of T3SS apparatus (*hrpF*, *hrpB1*, *hrcV*, *hrcN*, and *hrcU*) and effector genes (*xopL*, *xopR*, and *avrBs3*), as well as the T3SS key regulator genes (*hrpG* and *hrpX*) were determined by RT-qPCR. **b** Overexpression of *xrvB* reduced the transcription levels of the T3SS genes. Values are the means ± SD (n = 3 biological replicates). Differences were evaluated by Student's *t*-test (**$P < 0.01$)

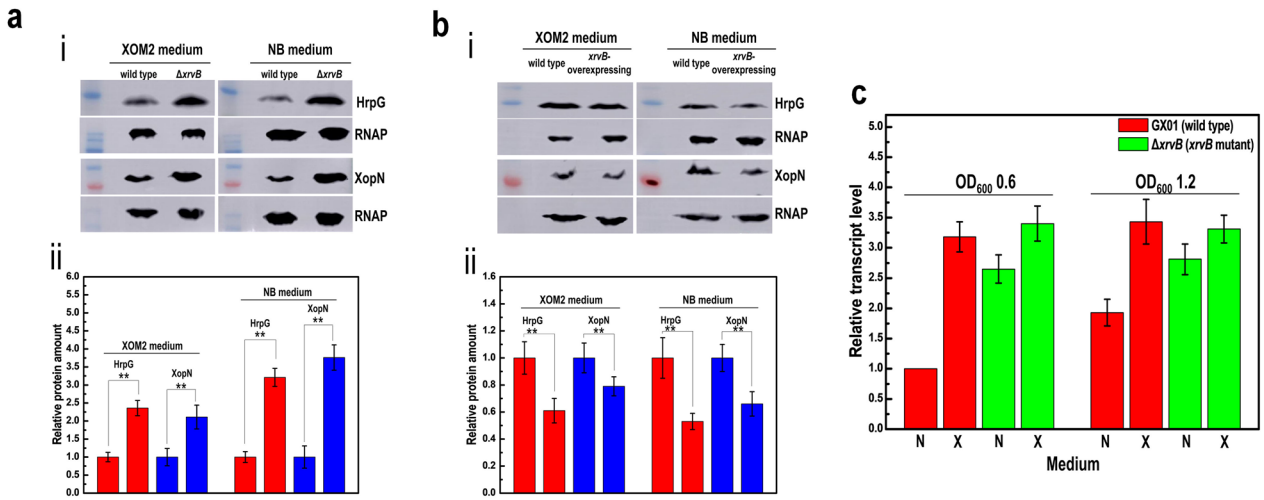

Fig. 3 XrvB is involved in the expression regulation of HrpG and XopN. **a** Deletion of *xrvB* enhanced the protein levels of HrpG and XopN. The *Xoc* strains GX01/HrpG::3 × Flag, Δ*xrvB*/HrpG::3 × Flag, GX01/XopN::3 × Flag, and Δ*xrvB*/XopN::3 × Flag were cultured in XOM2 or NB medium to mid-exponential growth phase (OD_{600} of 0.6), and total proteins were extracted. The proteins HrpG and XopN were detected using anti-Flag-tag antibody. RNAP served as a loading control. Proteins were quantified by Image J software. Band intensity of the proteins was normalized to RNAP levels. The mean value of the proteins in the wild-type strain was set to 1. Data are presented as means ± SD. $^{**}P < 0.01$, significant difference from the wild-type strain, using Student's *t*-test. **b** Overexpression of *xrvB* reduced the protein levels of HrpG and XopN. *Xoc* strains GX01/HrpG::3 × Flag/pBBad22K, GX01/HrpG::3 × Flag/pB*xrvB*, GX01/XopN::3 × Flag/pBBad22K, and GX01/XopN::3 × Flag/pB*xrvB* were cultured in XOM2 or NB to an OD_{600} of 0.6, and total proteins were extracted. Data presented are means ± SD (n = 3). The mean value of the proteins in GX01/pBBad22K strain was set to 1. $^{**}P < 0.01$, significant difference from the wild-type strain, using Student's *t*-test. **c** Deletion of XrvB significantly increased the transcription level of *hrpG* in the rich medium NB. Values given are the means ± SD (n = 3 biological repeats). N and X below the bar graph represent NB and XOM2 medium, respectively

indicate that overexpressing XrvB in *Xoc* undermines HrpG and XopN production. The above data reveal that *Xoc* XrvB negatively regulates the expression of T3SS.

Given that the expression of the *hrp* genes was induced in minimal media while was repressed in rich media, we determined whether deletion of XrvB affects the expression of *hrpG* in rich and minimal media by RT-qPCR analysis. *Xoc* strains were grown in NB and XOM2 media. The bacterial cells at mid (OD_{600} of 0.6) and late-exponential (OD_{600} of 1.2) growth phases were taken for the analysis. The result showed that the transcription levels of *hrpG* in the wild-type strain GX01 cultured in XOM2 were remarkably higher compared to NB, while the *hrpG* transcription levels in the *xrvB* deletion mutant Δ*xrvB* grown in XOM2 were only slightly higher relative to NB (Fig. 3c). This result suggests that *Xoc* XrvB plays a vital role in the regulation of *hrpG* expression in nutrition-rich media.

Xoc XrvB directly binds *hrpG* promoter and represses its transcription

We then explored how XrvB influenced *hrpG* expression. Based on the data that XrvB negatively affects the expression of *hrpG*, we inferred that XrvB possibly controls the transcription of *hrpG*. To verify this hypothesis, we first conducted electrophoretic mobility shift assay (EMSA). The 6 × His-tagged XrvB fusion protein (His-XrvB) was expressed and purified, and the 6-carboxyfluorescein (FAM)-labeled DNA fragment containing *hrpG* promoter region (spanning nucleotides from upstream 254-bp to downstream 42-bp relative to the start codon) was obtained by PCR-amplification from the *Xoc* wild-type strain GX01. As shown in Fig. 4a, His-XrvB caused a mobility shift of DNA probes spanning the promoter of *hrpG* and the shifted probe DNA increased following the increasing concentrations of XrvB protein (scale from 0 to 40 nM), demonstrating that XrvB physically interacted with *hrpG* promoter in vitro. This notion was confirmed by a competition assay using the cold DNA probes (unlabeled DNA). The result showed that the shifted bands was replaced by the unlabeled probes (Fig. 4a). Simultaneously, a 299-bp DNA fragment containing *rpfG* promoter region was used as a control. The result showed that no retarded band was observed when His-XrvB was added (data no shown). XrvA and XrvC proteins fused with 6 × His tag were also produced and used for EMSA with the labeled *hrpG* promoter region. As expected, no shifted band was observed under the tested conditions, indicating that XrvA and XrvC do not physically interact with the *hrpG* promoter in vitro (Additional file 1: Figure S3).

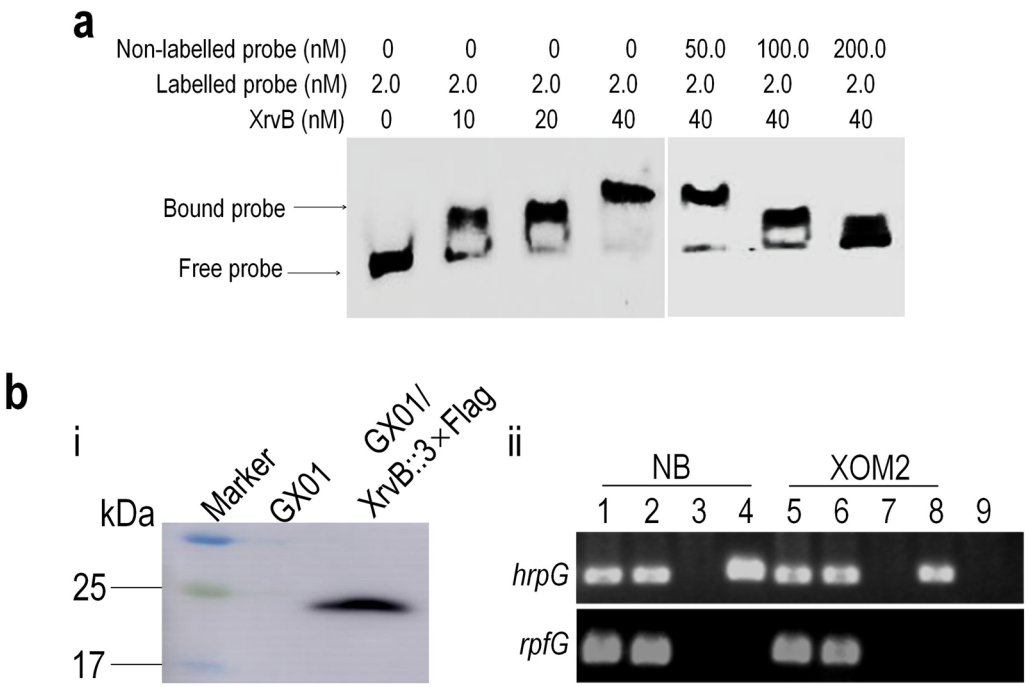

Fig. 4 XrvB directly binds to the *hrpG* promoter region. **a** Electrophoretic mobility shift assay showed XrvB protein interacted with the *hrpG* promoter region. The gel shift assay was carried out using the 6-carboxyfluorescein (FAM)-labeled DNA probe of the *hrpG* promoter and His-XrvB protein. The migrated DNA–protein complexes and free probe are indicated by arrows. **b** Chromatin immunoprecipitation (ChIP) assay showing that XrvB binds to the *hrpG* promoter region in vivo. The *Xoc* strain GX01/XrvB::3 × Flag was grown in NB and XOM2 media at an OD_{600} value of 0.3. Template DNA from a non-conjugated ChIP sample was used as the input control and DNA fragments containing *rpfG* promoter were amplified as a negative control. Lane 1 and 5 are GX01 total DNA (PCR efficacy control); lane 2 and 6 are the GX01/XrvB::3 × Flag total DNA (input control); lane 3 and 7 are the eluted DNA of GX01/XrvB::3 × Flag using anti-HA antibody (negative control); lane 4 and 8 are the eluted DNA of GX01/XrvB::3 × Flag using anti-Flag antibody; lane 9 is mock control

To verify whether XrvB binds *hrpG* promoter in vivo, we performed a chromatin immunoprecipitation (ChIP) assay. To this end, an *Xoc* strain (GX01/XrvB::3 × Flag) expressing the XrvB protein fused with a 3 × Flag-tag at its C-terminus was constructed. *Xoc* strains were grown in the nutrition-rich medium NB and the minimal medium XOM2 to OD_{600} of 0.3 for the ChIP assay. A Western blot assay confirmed that XrvB-Flag could be obtained from the strain GX01/XrvB::3 × Flag (Fig. 4b-i). The ChIP assay showed that using the eluted DNA from XrvB-Flag protein as template, *hrpG* promoter region could be amplified by the primer pair *hrpG*-chipF/R (Additional file 2: Table S2), but not by the control primer pair *rpfG*-chipF/R (Additional file 2: Table S2) for *rpfG* promoter (Fig. 4b-ii, lanes 4 and 8). These data indicate that XrvB binds *hrpG* promoter in *Xoc* cells.

The above data showed that XvrB negatively regulates *hrpG* expression via binding to its promoter region. To confirm this observation, the in vitro transcription assays were performed. A 433-bp template DNA fragment containing *hrpG* promoter region (comprising 233-bp upstream and 200-bp downstream DNA regions of the *hrpG* start codon) was incubated with RNA polymerase holoenzyme (RNAP) from *Escherichia coli* with increasing amounts of His-XvrB protein. In parallel, a 429-bp DNA fragment containing *rpfG* promoter (comprising 279-bp upstream and 150-bp downstream DNA sequences of the *rpfG* start codon) was used as a negative control. The result showed that when 0.5 U RNAP was added, the *hrpG* and *rpfG* transcripts could be observed. However, when XvrB protein was added, the *hrpG* transcripts, but not *rpfG*, were remarkably decreased and the decreasing levels of *hrpG* transcripts were negatively correlated with the increased amount of XvrB (from 5 to 20 nM) (Fig. 5a). This result demonstrates that XvrB represses the transcription of *hrpG* in vitro.

XrvB production is repressed and its occupancy at *hrpG* promoter region is decreased in *hrp*-inducing minimal medium

The occupancies of XrvB at *hrpG* promoter in *Xoc* cells grown in NB and XOM2 media were further examined by quantitative PCR (qPCR). The strain GX01/XrvB::3 × Flag was cultured in NB and XOM2. Bacterial cells of a volume corresponding to the density of OD_{600} of 1.0 were taken at the early- (OD_{600} of 0.3), mid- (OD_{600} of 0.6), and

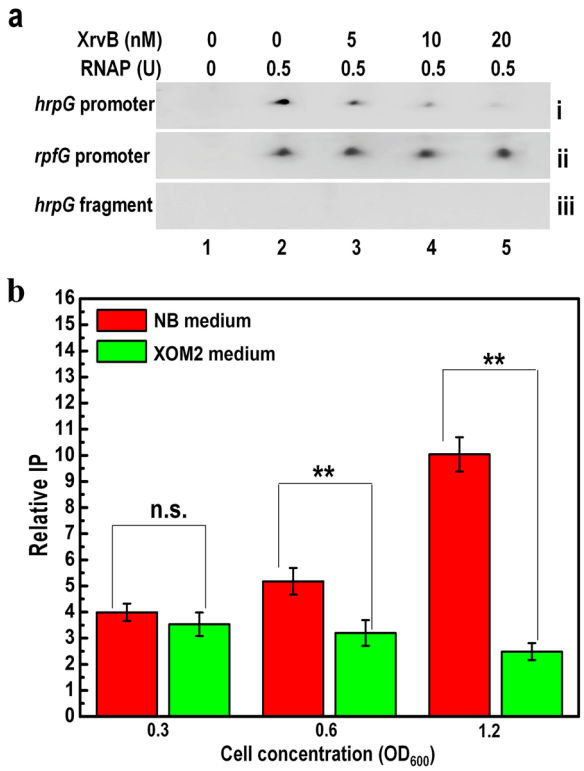

Fig. 5 XrvB repressed *hrpG* transcription and its occupancy at the *hrpG* promoter region in a rich medium. **a** In vitro transcription assay showing that XrvB repressed the transcription of *hrpG*. RNA was generated from a 433-bp template DNA fragment containing *hrpG* promoter using *E. coli* RNA polymerase (RNAP) holoenzyme. A 429-bp template DNA fragment containing the *rpfG* promoter and a 208-bp template DNA fragment of *hrpG*-coding sequence were used as a control. Lane 1, template DNA alone; Lane 2, template DNA with RANP; Lanes 3–5, template DNA with RANP and 5, 10 and 20 nM His-XrvB. **b** ChIP and qPCR assays demonstrate that XrvB occupancy at the *hrpG* promoter region increased in the cells grown in the nutrient-rich medium NB. Data are presented as means ± SD (n = 3). Differences were evaluated using Student's *t*-test (**$P < 0.01$; n.s. no significance at $P \leq 0.05$)

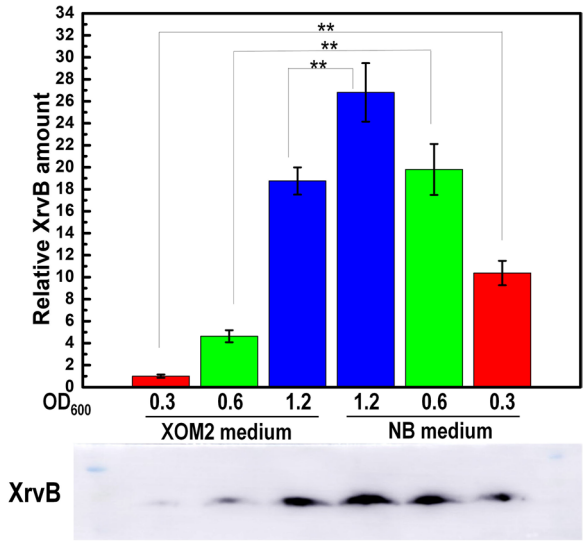

Fig. 6 Western blot and densitometry analysis of XrvB protein abundance. Total protein was extracted from *Xoc* wild-type cells expressing XrvB protein fused with 3 × Flag cultured in XOM2 and NB medium. Data are presented as means ± SD (n = 3). The mean value of XrvB protein levels in bacterial cells cultured in XOM2 at OD_{600} of 0.3 was set equal to 1. Significance was determined by Student's *t*-test. **$P < 0.01$

late-exponential (OD_{600} of 1.2) growth phases, respectively, and the immunoprecipitated (IP) DNA was prepared and used as template for qPCR analysis. Template DNA from a non-conjugated ChIP sample was used as an input control. The quantity of IP DNA was calculated as the percentage of the DNA present in the input sample. The relative IP was calculated by standardizing the IP of each sample by the IP of the corresponding mock ChIP. As shown in Fig. 5b, the IP values from the cells grown in NB after the mid-exponential growth phase are significantly higher than that from the cells grown in XOM2. These data implied that XrvB occupancy at *hrpG* promoter was significantly higher in the cells cultured in the nutrition-rich medium than the minimal medium.

The above results suggest that the expression of XrvB was induced in a nutrition-rich medium and repressed in a minimal medium. To verify this, the strain GX01/XrvB::3 × Flag was grown in NB and XOM2, respectively. Bacterial cells of a volume corresponding to the density of 1.0 OD_{600} unit were taken at the early- (OD_{600} of 0.3), mid- (OD_{600} of 0.6), and late-exponential (OD_{600} of 1.2) growth phases, and the production of XrvB was assessed by the western blot assay. The result revealed that the levels of XrvB-Flag were significantly elevated in the cells cultured in the nutrition-rich medium NB compared to the minimal medium XOM2 in all the tested time-points, and XrvB level was increased in the cells cultured in both media with the bacterial growth course (Fig. 6). Taken together, the above data indicate that XrvB production is reduced and its occupancy at *hrpG* promoter region is decreased in the *hrp*-inducing minimal medium XOM2.

Xoc XrvB plays a positive role in full virulence

The above results demonstrated that XrvB suppressed the expression of T3SS by direct reducing *hrpG* transcription. To explore the role of XrvB in the virulence of *Xoc*, we tested the pathogenicity of *xrvB* deletion strain. The strain was inoculated on the leaves of susceptible rice plants and the disease symptoms were observed at 14 days after inoculation. Interestingly, the lesion length caused by the *xrvB* deletion mutant Δ*xrvB* was significantly shorter compared to the wild type. The

disease symptoms produced by the complemented strain C*ΔxrvB*, and the *xrvA* and *xrvC* deletion mutants *ΔxrvA* and *ΔxrvC* were similar to that provoked by the wild-type strain (Fig. 7a). These results revealed that deletion of XrvB but not XrvA and XrvC could reduce the pathogenicity of *Xoc*.

The effect of deletion of XrvB on the proliferation of the pathogen in host tissues was further assessed. To do this, the bacterial cell numbers of *ΔxrvB* and control strains (GX01 and C*ΔxrvB*) in infected rice leaves were determined at each day of the first 7 days after inoculation. Results revealed that the cell number of the mutant *ΔxrvB* that recovered from leaf tissues within the inoculated area was 10- to 100-fold less compared to the wild-type strain up to 4 days post-inoculation (Fig. 7b-i). The complemented strain C*ΔxrvB* showed similar cell numbers to the wild-type strain (Fig. 7b-i). These data suggested that loss of XrvB impacts *Xoc* growth at early infection stage. The growth rate of the XrvB deletion mutant in the nutrition-rich medium NB was also examined. The result showed that *ΔxrvB* displayed a reduced growth rate compared to the wild type throughout the lag and exponential phases (Fig. 7b-ii), indicating that *Xoc* XrvB is indispensable for pathogen growth.

Xoc XrvB is involved in cell motility and stress tolerance

The reduced pathogenicity of XrvB-deficient mutant implies a possibility that XrvB is involved in other cellular processes required for the full pathogenicity of *Xoc*, such as the production of extracellular enzymes and polysaccharide (EPS), cell motility, and stress tolerance. To validate this hypothesis, we assessed the production of EPS, extracellular protease and endoglucanase, swimming and swarming motility, and tolerance to

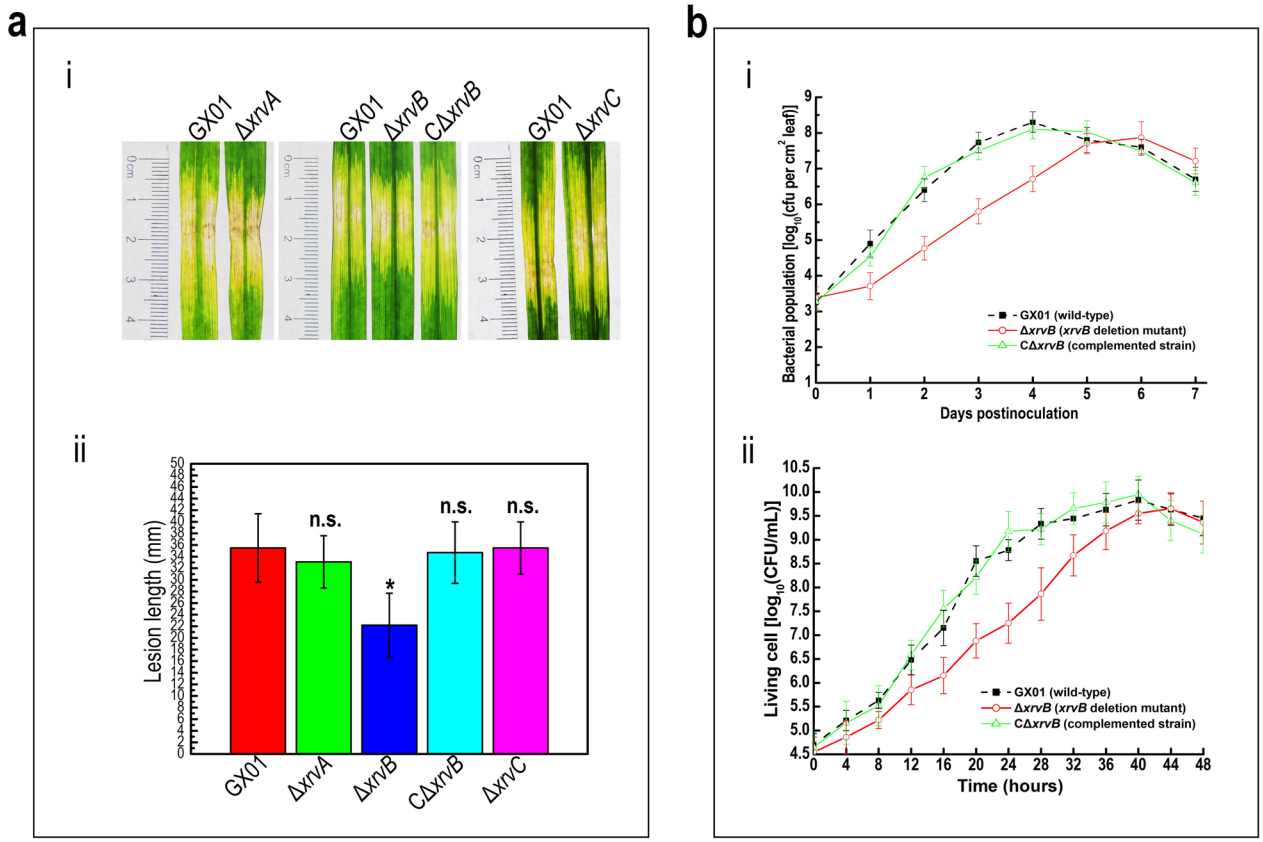

Fig. 7 XrvB is required for the full virulence of *Xoc*. **a** Virulence test of *Xoc* strains. Six-week-old susceptible rice plants (*Oryza sativa* L. ssp. *Japonica* cultivar *Nipponbare*) were inoculated with bacterial suspensions of the *Xoc* strains by the leaf-infiltrating method. Symptoms were recorded at 14 dpi and lesion lengths were scored. Values are the mean ± SD (n = 25). Significance was determined by ANOVA and Dunnett's post hoc test for comparison to the wild type. *$P < 0.05$; n.s., not significant. The experiment was repeated three times with similar results. **b** Growth test of *Xoc* strains *in planta* and in complex media NB. The *Xoc* wild-type strain GX01, the *xrvB* deletion mutant *ΔxrvB*, the complemented strain C*ΔxrvB* were infiltrated into the leaves of rice. Bacterial colony-forming units (CFU) were counted after incubation for 3 days. Data are shown as the mean ± SD (n = 3 biological repeats). For the growth assay in media, the *Xoc* strains were inoculated into 100 mL NB medium with the same final density of 0.01 (OD_{600}). Samples were taken in triplicate at intervals of 4 h, diluted, and plated on NA plate. Bacterial CFU were counted after incubation for 3 days. Data are shown as the mean ± SD (n = 3 biological repeats)

several environmental stress agents, including sodium dodecyl sulphate (SDS), phenol, NaCl, and $CuSO_4$.

The results showed that the EPS production and activities of extracellular protease and endoglucanase produced by the *xrvB* deletion mutant strain Δ*xrvB* were similar to that produced by the wild type under the tested conditions (Additional file 1: Figure S4). However, both swimming and swarming motilities of Δ*xrvB* were significantly attenuated compared to the wild type (Fig. 8a). Notably, the complemented strain CΔ*xrvB* showed significantly increased swarming ability while its swimming ability was not remarkably altered, compared to the wild type (Fig. 8a). As shown in Fig. 8b, the tolerance of Δ*xrvB* to all the stress agents was remarkably compromised compared to the wild type, while the complemented strain CΔ*xrvB* showed similar tolerance to the tested agents as wild type. Taken together, these data demonstrated that XrvB plays a positive role in cell motility and stress tolerance.

Discussion

Our study revealed that the *Xoc* H-NS protein XrvB is a global regulator in various cellular processes, including bacterial growth, the T3SS-asscoaited gene expression, cell motility, and stress tolerance. It is consistent with the conclusion from previous studies that a bacterial H-NS protein can regulate multiple different cellular processes that are associated with cell growth, adaptation to environmental challenges, and virulence factor production (Bertin et al. 2001; Tendeng and Bertin 2003; Müller et al. 2010).

In this work, we mainly focused on the regulation mechanism of XrvB on the expression of T3SS-asscoatiated genes. T3SS is an essential virulence determinant in many Gram-negative bacterial pathogens including *Xanthomonas* spp.. Great efforts have been made to uncover the molecular mechanism of the regulation for the *hrp* genes that encode the T3SS in *xanthomonads* spp. In addition to HrpG, HrpX, XrvA, XrvB, and XrvC, a number of proteins involved in *hrp* gene expression have been identified, including the HrpG upstream regulators HpaS,

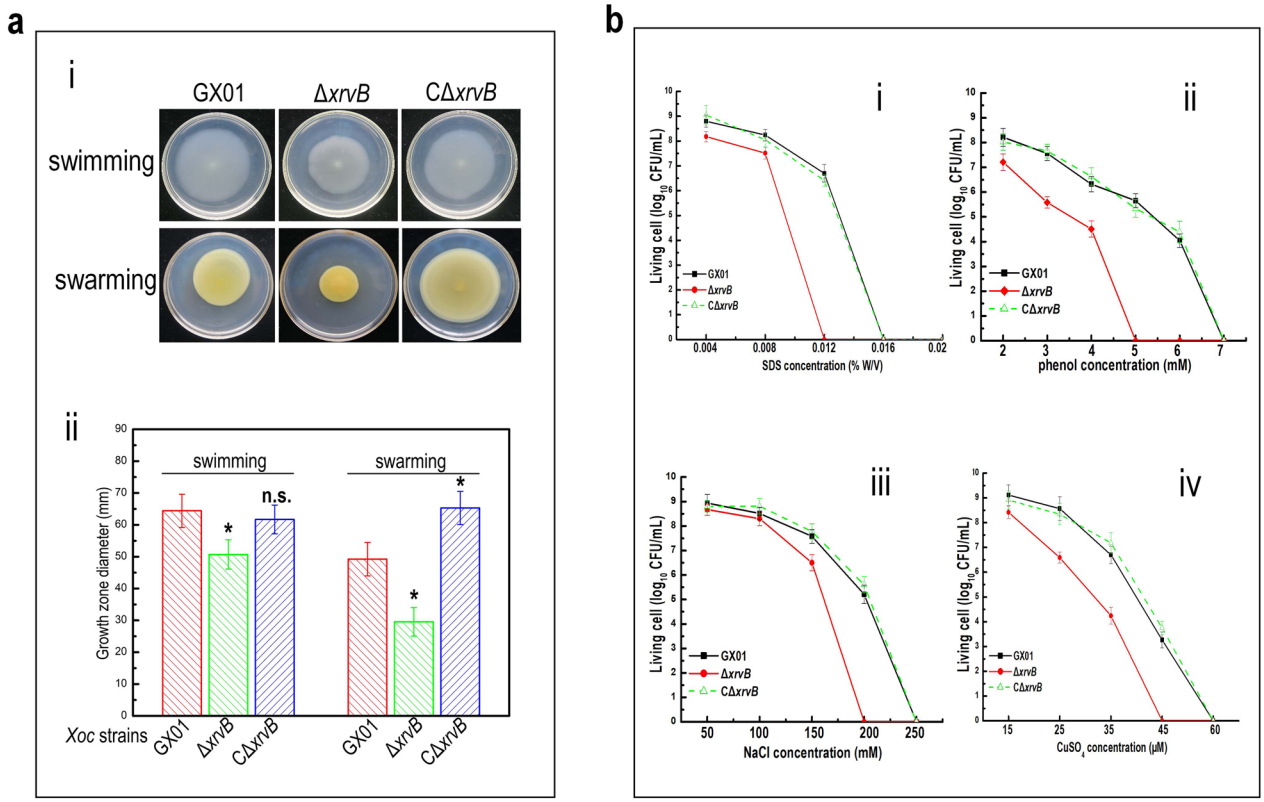

Fig. 8 XrvB plays positive impacts on cell motility and stress tolerances. **a** Cell motility test of *Xoc* strains. Two microliters of *Xoc* culture suspension (OD_{600} of 1.0) were stabbed into 'swimming' plates or inoculated onto "swarming" plates followed by incubation for 4 days. Data shown are the mean ± SD (n = 15). Significance was determined by ANOVA and Dunnett's post hoc test for comparison to the wild type. *$P < 0.05$; n.s., not significant. **b** Stress tolerance test of *Xoc* strains. Survival experiments were performed by subculturing strains overnight on fresh NA agar plates supplemented with different concentrations of SDS (i), phenol (ii), NaCl (iii), and $CuSO_4$ (iv). The surviving bacterial colonies on the plates were counted after incubation for 3 days. Values given are the means ± SD (n = 3 biological repeats)

HpaR1/YtrA, RsmA, GamR, Lon, and DksA (Büttner and Bonas 2010; An et al. 2020; Teper et al. 2021). HpaS, identified from crucifer black rot pathogen *X. campestris* pv. *campestris* (*Xcc*), is a membrane-bound histidine kinase sensor, which forms a two-component signal transduction system with HrpG and activates HrpG activity via phosphorylation (Li et al. 2014). HpaR1/YtrA is a GntR-family transcriptional regulator, identified from *Xcc* and the citrus canker pathogen *X. citri* subsp. *citri* (*Xcci*), which negatively regulates the expression of *hrpG* in both minimal and rich media but positively regulates the gene expression *in planta* (An et al. 2011; Zhou et al. 2017). RsmA is a post-transcriptional regulator. In *Xcci*, it binds to the 5'UTR of *hrpG* mRNA and consequently promotes its translation (Andrade et al. 2014). GamR is a LysR-type galactose metabolism regulator. It was reported that in *Xoo*, GamR regulates *hrp* gene expression through transcriptional activation of *hrpG* in minimal media; however, mutation of *gamR* did not significantly alter the virulence of *Xoo in planta* (Rashid et al. 2016). In *Xcci*, the Lon protease degrades HrpG protein and controls the stability of HrpG (Zhou et al. 2018). DksA, a transcription factor of DksA/TraR superfamily, is a stringent response regulator. It was shown that deletion of *dksA* led to a significant reduction of the expression of *Xcci hrpG* (Zhang et al. 2019). Notably, of these proteins, only HpaR1/YtrA functions in suppressing *hrpG* expression (in media). However, whether the negative regulation is direct or indirect still remains elusive, as in vitro EMSA and in vivo ChIP assays did not show a physical interaction of HpaR1/YtrA and *hrpG* promoter (An et al. 2011; Zhou et al. 2017). To the best of our knowledge, XrvB is the second identified protein with negative regulatory function on *hrpG* expression in *Xanthomonas*. Importantly, our EMSA, ChIP, and in vitro transcription results reveal that *Xoc* XrvB binds to the promoter of *hrpG* and represses its transcription. Previously, Kametani-Ikawa et al. reported that *Xoo* XrvB negatively regulated the expression of *hrp* genes, including *hrpG*. However, no physical interaction between *Xoo* XrvB and *hrpG* promoter was observed in the EMSA assay, although XrvB could bind to a DNA fragment containing the *bla* promoter region (Kametani-Ikawa et al. 2011). Based on these findings, we concluded that the regulation of XrvB to *hrpG* expression might require another unknown factor(s) in *Xoo* (Kametani-Ikawa et al. 2011). Notably, the XrvB proteins in *Xoc* and *Xoo* are very similar (95.4% identities). The discrepancy of the two proteins in regulating *hrpG* expression needs further investigations.

Previous studies have shown that in *Xanthomonas*, the expression of *hrpG* is suppressed in nutrient-rich media but induced in plants and the minimal media (Büttner and Bonas 2010; Teper et al. 2021). However, the mechanism is unclear, although many proteins in regulating *hrpG* expression have been identified. Our data suggest that in *Xoc*, XrvB plays an important role in the expression of *hrpG*. RT-qPCR analysis showed that the transcription level of *hrpG* in the wild-type cells grown in the *hrp*-inducing minimal medium XOM2 was much higher compared to the nutrient-rich medium NB; however, in the *xrvB* deletion mutant that was grown in XOM2, the *hrpG* transcription level was only slightly higher than that in NB (Fig. 3c). Furthermore, the production of XrvB in the *Xoc* cells cultured in XOM2 was significantly reduced compared to NB (Fig. 6). Accordingly, the XrvB occupancy at *hrpG* promoter region is remarkably decreased in the cells grown in XOM2 than NB (Fig. 5b). These data strongly suggest that XrvB is a determinative factor controlling the expression of HrpG in *Xoc* (Figs. 4, 5). The expression level of HrpG is negatively correlated with the content of XrvB in *Xoc* cells. At this point, we do not know what factor(s) in the media controls the expression of XrvB. Further identification of the factor(s) will greatly facilitate our understanding of the molecular mechanisms governing the T3SS expression of *Xoc* under different growth conditions.

Notably, although deletion of XrvB in *Xoc* did not impair HR induction (Fig. 1), the XrvB-deficient mutant displayed a significant reduction in pathogenicity (Fig. 7a). The reason is likely because *Xoc* XrvB also positively affects bacterial growth, cell motility, and stress tolerance, in addition to suppressing *hrpG* expression. The XrvB-deficient mutant exhibited a significant impairment in cell growth (Fig. 7b), swimming and swarming motility (Fig. 8a), as well as stress tolerance (Fig. 8b). Further studies on the molecular mechanisms by which XrvB regulates cell motility and stress tolerance are of great value. As mentioned above, it was reported that both XrvA and XrvC positively regulate *hrp* gene expression in *Xoo*. Deletion of XrvA or XrvC significantly reduced the HR induction and virulence of *Xoo* (Feng et al. 2009; Liu et al. 2016). However, our work showed that deletion of either XrvA or XrvC in *Xoc* did not lead to an obvious diminution in HR induction and virulence on plants (Additional file 1: Figure S2 and Fig. 7a), although they share very high identity. The function of XrvA and XrvC in *Xoc* remains to be investigated in the future.

Conclusions

In conclusion, our work demonstrated that the *Xoc* XrvB represses the expression of the key *hrp* gene regulator *hrpG*. The expression level of XrvB in the *Xoc* cells cultured in a nutrient-rich medium is significantly higher compared to a *hrp*-inducing minimal medium, and the expression level of HrpG is negatively correlated with the content of XrvB in *Xoc* cells. Furthermore, the

occupancy of XrvB at *hrpG* promoter is positively correlated with the content of XrvB protein in *Xoc* cells. Our data strongly suggest that XrvB is a determinative factor controlling the expression of HrpG in *Xoc*. Although the factor(s) modulating the expression of XrvB remains to be identified, our finding provides a better understanding of the molecular mechanisms governing the expression of the essential virulence determinant T3SS in *Xoc*.

Methods

Bacterial strains, plasmids, culture media, and growth conditions

Strains and plasmids used in this study are listed in Additional file 2: Table S1. *Xoc* strains were grown at 28 °C in NB medium (per litre:1 g yeast extract, 3 g beef extract, 5 g polypeptone, 10 g sucrose), NA (NB with 15 g agar per litre), or the minimal medium XOM2 (Tsuge et al. 2002). *E. coli* strains were grown in LB (Luria–Bertani) medium (per litre: 5 g yeast extract, 10 g NaCl, 10 g tryptone) or on LB agar plates (LB with 15 g agar per litre) at 37 °C. Antibiotics were used at the following concentrations: kanamycin (Kan) at 25 μg/mL, rifampicin (Rif) at 50 μg/mL, ampicillin (Amp) at 100 μg/mL, spectinomycin (Spc) at 50 μg/mL, and tetracycline (Tet) at 5 μg/mL for *Xanthomonas* strains or 15 μg/mL for *E. coli* strains.

RT-qPCR assays

The nucleic acid manipulations followed the procedures described by Sambrook et al. (1989). Conjugation between *Xoc* and *E. coli* strains was performed as described by Turner et al. (1985). The restriction endonucleases, T4 DNA ligase and *Pfu* DNA polymerase were provided by Promega (Shanghai, China). Total RNA was extracted from cultures of *Xoc* strains with a total-RNA extraction kit (Invitrogen, Waltham, MA, USA) and cDNA was generated using a cDNA synthesis kit (Invitrogen). For RT-qPCR, the obtained cDNA was diluted and used as a template with selected primers for target genes (Additional file 2: Table S2). RT-qPCR was performed in qPCR thermal cycler (Analytik jena qTOWER2.0, Jena, Germany). Reactions included ChamQ universal SYBR qPCR master mix (Vazyme), corresponding primers (Additional file 2: Table S2) and cDNA templates. Reactions with blank template were used as negative controls. The melting curve analysis was performed at temperature ranging from 60 °C to 95 °C by increasing 0.5 °C at each second. The relative mRNA level was calculated with respect to the level of the corresponding transcript in the wild-type strain GX01 (equaling 1). The expression level of the 16S rRNA gene was used as an internal standard. The RT-qPCR tests were performed in triplicate.

Construction of mutant strains

The construction of an in-frame deletion mutant of *xrvA*, *xrvB*, or *xrvC* in *Xoc* was carried out using a previously described method (Cui et al. 2018). For *xrvA*, 557-bp upstream and 622-bp downstream fragments of the *xrvA* coding region were PCR-amplified using the corresponding primers (Additional file 2: Table S2). The two fragments were ligated together and cloned into the vector pK18*mobsacB* (Schäfer et al. 1994), and the obtained plasmid (pKΔ*xrvA*) was introduced into the *Xoc* strain GX01. Mutants were selected and confirmed by PCR and named as Δ*xrvA*. Similarly, for *xrvB* deletion mutant construction, 617-bp upstream and 611-bp downstream fragments amplified by PCR were cloned into pK18*mobsacB* to generate the recombinant plasmid pKΔ*xrvB* (Additional file 2: Table S2). The recombinant plasmid was introduced into *Xoc* strain GX01, resulting in mutant strain Δ*xrvB* (Additional file 2: Table S2). For the *xrvC* deletion mutant (Δ*xrvC*) construction, the recombinant plasmid pKΔ*xrvC* (Additional file 2: Table S2) which is derived from the 512-bp upstream and 516-bp downstream fragments flanking *xrvC* coding sequence cloned into the plasmid pK18*mobsacB*, was introduced into *Xoc* strain GX01.

For complementation of the Δ*xrvB*, Δ*xrvB*, and Δ*xrvC* mutant, the full length of *xrvA*, *xrvB*, and *xrvC* was amplified by PCR from the total DNA of *Xoc* strain GX01 with primers C*xrvA*-F/R, C*xrvB*-F/R, and C*xrvC*-F/R (Additional file 2: Table S2), respectively. Primers were modified to give *Hin*dIII- or *Xba*I-compatible ends. The amplified fragments were cloned into the low-copy-number plasmid pLAFR3 (Staskawicz et al. 1987). The obtained plasmids pLC*xrvA*, pLC*xrvB*, and pLC*xrvC* (Additional file 2: Table S1) were introduced into the corresponding mutants by tri-parental conjugation to generate complemented strains CΔ*xrvA*, CΔ*xrvB*, and CΔ*xrvC* (Additional file 2: Table S1).

For overexpression of *xrvA*, *xrvB*, or *xrvC* in *Xoc*, DNA fragments of *xrvA*-, *xrvB*-, or *xrvC*-coding sequences amplified using the corresponding primer sets (Additional file 2: Table S2) were cloned into the broad-host-range expression vector pBBad22K (Sukchawalit et al. 1999), and the obtained recombinant plasmids pB*xrvA*, pB*xrvB*, and pB*xrvB* were introduced into the *Xoc* strain GX01, respectively, which are the strains GX01/pB*xrvA*, GX01/pB*xrvB*, and GX01/pB*xrvC* (Additional file 2: Table S1).

Construction of the strains with Flag-tagged proteins

Xoc strains chromosomally encoding the proteins fused with a 3×Flag-tag at the C-terminus were constructed using the method previously described (Li et al. 2022). To

construct a strain expressing XrvB-Flag for ChIP assays and western blotting, a 504-bp DNA fragment which was composed of 459-bp XrvB-coding sequence and 45-bp Flag-coding sequence was generated by PCR amplification using the genomic DNA of strain GX01 as template and the primer set L*XOCgx_0907*-FlagF/R (Additional file 2: Table S2). Simultaneously, a 464-bp DNA fragment which was composed of 41-bp Flag-coding sequence, the 3-bp stop codon of *xrvB*, and 420-bp downstream of the *xrvB* stop codon was generated by PCR amplification using the primer set R*XOCgx_0907*-FlagF/R (Additional file 2: Table S2). The two fragments were jointed using overlap extension PCR, and the resulting recombinant fragment was cloned into the suicide plasmid pK18*mobsacB* (Additional file 2: Table S1). The resulting recombinant plasmid was named as pK*xrvB*::*Flag* (Additional file 2: Table S1) and the plasmid was further introduced into *Xoc* strain GX01 by conjugation. The transconjugants were screened on selective agar plates and were confirmed by DNA sequencing. This constructed variant strain was named as GX01/XrvB::3×Flag (Additional file 2: Table S1). Similarly, to construct *Xoc* strains expressing HrpG-Flag or XopN-Flag for Western blot assays, a sequence encoding an in-frame 3×Flag epitope at the C-terminus of HrpG or XopN was obtained by PCR amplification with the corresponding primer sets (L*hrpG*-FlagF/R and R*hrpG*-FlagF/R for HrpG::3×Flag, L*xopN*-FlagF/R and R*xopN*-FlagF/R for XopN::3×Flag) (Additional file 2: Table S2). These obtained recombinant fragments were cloned into the suicide vector pK18mob*sacB*, respectively. The resulting recombinant plasmids, named pK*hrpG*::*flag* and pK*xopN*::*flag* (Additional file 2: Table S1), were introduced into the *Xoc* wild-type strain GX01 and *xrvB* deletion mutant Δ*xrvB*, respectively. The obtained *Xoc* wild-type strains chromosomally encoding fused protein HrpG-Flag or XopN-Flag were named as GX01/HrpG::3×Flag or GX01/XopN::3×Flag, and the *xrvB* deletion mutant expressing these fused protein were named as Δ*xrv*/HrpG::3×Flag or Δ*xrv*/XopN::3×Flag (Additional file 2: Table S1).

ChIP and promoter occupancy assays

ChIP and promoter occupancy assays were performed as previously described (Wang et al. 2012; Liu et al. 2019), with minor modifications. In brief, the GX01/XrvB::3×Flag reporter strain was grown in XOM2 or NB medium for an appropriate period of time and cross-linked using formaldehyde. Samples of a volume (50 mL) corresponding to 1.0 OD_{600} unit were taken at different time points and centrifuged, then cells were lysed by sonication and debris was removed. For each ChIP sample, 50 μL of anti-Flag (agarose conjugated) was added to 3.5 mL of the bacterial lysates and incubated overnight. Unbound DNA fragments were washed and the bound DNA fragments and proteins were eluted by 0.25 M glycine (pH 2.5). The eluted proteins were resolved by SDS-PAGE and Western blotting, and the immunoprecipitated (IP) DNA (eluted DNA) were used as templates for PCR or qPCR analysis. Non-conjugated ChIP sample was used as a reference.

To quantitate promoter occupancy by XrvB-Flag, qPCR was conducted using the ChamQ universal SYBR qPCR master mix (Vazyme) with primer set *hrpG*-chipF/R on a real-time PCR thermal cycler (Analytik jena qTOWER2.0; Jena). The quantity of IP DNA (eluted DNA) was calculated as the percentage of the DNA present in the input DNA (10 μL sample taken prior to IP) using the formula $IP = 2^{CtInput-CtIP}$, where Ct is the fractional threshold cycle of the input and IP samples. The relative IP was calculated by normalizing the IP to a mock ChIP using the anti-HA-tag monoclonal antibody (Solarbio).

Western blotting

Western blotting followed the procedure described by Sambrook et al. (1989). Bacterial proteins separated by SDS-PAGE gel were electrotransferred onto a polyvinylidene difluoride (PVDF) membrane (Millipore, Billerica, MA, USA). After blocking with 1% milk, the proteins in the membrane were incubated with the 1:2500 diluted anti-Flag-tag mouse monoclonal antibody (Solarbio) as the primary antibody, followed by washing with Tris-buffered saline with Tween buffer (Tris 20 mM, NaCl 0.3 M, Tween 20 0.08%). The diluted 1:2500 horseradish peroxidase (HRP)-conjugated goat anti-mouse immunoglobulin G (IgG) was used as the secondary antibody. The luminescence signal was detected according to the manufacturer's instructions. For a loading control, proteins were probed with the anti-RNAP β-antibody (EPR18704; Abcam) at 1:2000 dilution as primary antibody, and the HRP-conjugated goat anti-rabbit IgG H&L (31,460; Thermo Scientific Waltham, MA, USA) at 1:5000 dilution as secondary antibody. The intensities of the Western blotting bands were quantified using ImageJ.

Overexpression and purification of His-XrvB protein

To produce the 6×His-tagged XrvB (6×His::XrvB), the 462-bp *xrvB* coding sequence was PCR-amplified using primers pQE0907-F/R (Additional file 2: Table S2). The obtained DNA fragments were cloned into the expression vector pQE-30a. The resulting recombinant plasmid named as pQE-30a-XrvB (Additional file 2: Table S1) was transformed into the *E. coli* strain BL21. The obtained recombinant strain was cultured and induced by isopropyl *β*-d-thiogalactopyranoside (IPTG), and then the cells

were collected and the fusion protein was purified using Ni–NTA resin (Qiagen).

Electrophoretic mobility shift assay (EMSA)

EMSAs were performed as previously described (Su et al. 2016). Briefly, a 296-bp DNA fragment comprising 254-bp upstream and 42-bp downstream sequences of *hrpG* start codon was amplified by PCR using the FAM-labeled primers *hrpG*-emF/R (Additional file 2: Table S2). The labeled DNA fragment (1.0 nM) was mixed with the purified His-XrvB (or His-XrvA and His-XrvC) protein in 20 μL of binding buffer that contains sonicated salmon sperm DNA and bovine serum albumin, and incubated at 30 °C for 20 min. Samples were then loaded onto a 6% polyacrylamide-Tris-borate-EDTA gel, and was visualized after electrophoresis.

In vitro transcription assays

In vitro transcription assays were performed as previously described (Su et al. 2016). 433-bp DNA fragments containing the promoter of *hrpG* (233-bp upstream and 200-bp downstream fragments of the *hrpG* start codon) was acquired using PCR with the primer set *hrpG*-ivtF/R (Additional file 2: Table S2). His-XrvB protein and DNA fragments were incubated 30 min at room temperature in transcription buffer. Then, a NTP mixture (250 μM each of ATP, CTP and GTP, 250 μM biotin-16-UTP) and 0.5 U of *E. coli* RNA polymerase holoenzyme (New England BioLabs, Ipswich, MA, USA) were added to initiate the transcription. After incubation at 28 °C for 30 min, the reactions were terminated and the transcription products were analyzed by electrophoresis. The transcripts obtained were visualized using a phosphor imager screen (GE AI600).

Pathogen inoculation assays

The pathogenicity of *Xoc* on susceptible rice plants (*Oryza sativa* L. ssp. *Japonica* cultivar *Nipponbare*) was tested by the infiltrating method as previously described (Li et al. 2017, 2023), with minor modification. Briefly, *Xoc* wild-type strain and its derivatives were grown at 28 °C in NB medium for 24 h, and the cells were collected and re-suspended in sterile ultrapure water to a concentration of OD_{600} of 0.3 (approximately 1.0×10^8 CFU/mL). The re-suspended bacterial cells were inoculated onto six-week-old leaves of rice plant under relevant conditions. Symptoms were recorded by photography and the disease lesion lengths were measured at 14 days post-inoculation.

The growth of bacteria in rice leaves was measured by homogenizing a group of five samples in 9 mL ultrapure water. For each sample, three 0.4 cm^2 leaf discs were excised from each infiltrated area at indicated time intervals. Diluted homogenates were plated on selective NA plates with corresponding antibiotics, and bacterial colony-forming units (CFU) were counted after incubation for 3 days.

The HR test of *Xoc* was conducted as our previous description (Li et al. 2017). Briefly, *Xoc* cells from cultures were washed and re-suspended in sodium phosphate buffer (SPB, 5.8 mM Na_2HPO_4 and 4.2 mM NaH_2PO_4, pH 7.0) to an OD_{600} of 0.5 (5×10^8 CFU/mL). Bacterial suspensions were infiltrated into the mesophyll tissue of greenhouse-grown *Nicotiana benthamiana* leaves, and the symptoms were observed at 24, 36, and 48 h after infiltration. Meanwhile, the electrolyte leakage was determined by measuring the conductivity of the infiltrating spot in *N. benthamiana* leaves.

For RT-qPCR analysis of bacterial gene expression *in planta*, two-week-old rice seedlings (cultivar *Nipponbare*) were inoculated with the suspension of *Xoc* strains at a concentration of OD_{600} of 0.5 by infiltration. For each plant, the second and third leaves were used. The infiltrated leaf part was collected 24 h after inoculation and total RNA was extracted. The expression pattern of T3SS-related genes in plant infection were further examined using RT-qPCR, as previously described (Liao et al. 2019).

Extracellular polysaccharide and enzyme assays

EPS and extracellular enzyme assays were performed as previously described (Tang et al. 1991; Su et al. 2016). Briefly, to examine the EPS production, *Xoc* strains were spotted onto NA with 2% sucrose and grown for 5 days. For quantification of EPS production, *Xoc* strains were cultured in 100 mL NB broth containing 4% sucrose at 28 °C with shaking at 200 rpm for 3 days. For examination of the activity of the extracellular enzymes endoglucanase (cellulase) and protease, strains on NA plates containing carboxymethylcellulose (for endoglucanase) or skim milk (for protease) were incubated at 28 °C for 48 h. For quantification of enzymes, bacterial cells were cultured in NB medium for 24 h and adjusted to the same concentration.

Stress tolerance assay

The tolerance of *Xoc* strains to several environmental stresses, including SDS, the organic solvent phenol, hyperosmotic challenge NaCl, and heavy metal salt $CuCl_2$, was tested using the minimal inhibitory concentration (MIC) method (Li et al. 2020). Briefly, 100 μL of the diluted cultures (OD_{600} of 1.0) of *Xoc* strains were plated on NA plates supplemented with different concentrations of each reagent. The surviving colonies on the plates were counted after 3 days of incubation at 28 °C.

Motility assay

Swimming and swarming motilities of *Xoc* were determined as previously described (Li et al. 2020). Briefly, two microliters of bacterial suspension (OD_{600} of 1.0) was placed onto 0.28% agar plates that are composed of 0.03% Bacto peptone and 0.03% yeast extract (for swimming), or spotted on NB plates containing 2% glucose and 0.6% agar (for swarming). The diameters of the area occupied by the bacterial cells were measured at 4 days after incubation at 28 °C.

Abbreviations

ANOVA	Analysis of variance
Amp	Ampicillin
CFU	Colony-forming units
ChIP	Chromatin immunoprecipitation
EMSA	Electrophoretic mobility shift assay
EPS	Extracellular polysaccharide
FAM	6-Carboxyfluorescein
H-NS	Histone-like nucleoid-structuring
HR	Hypersensitive reaction
hrp	Hypersensitive response and pathogenicity
IP	Immunoprecipitated
Kan	Kanamycin
OD_{600}	Optical density at 600 nm
Rif	Rifampicin
RNAP	RNA polymerase holoenzyme
RT-qPCR	Reverse transcription-quantitative real-time PCR
SPB	Sodium phosphate buffer
Spc	Spectinomycin
T3SS	Type III secretion system
Tet	Tetracycline
Xcc	*Xanthomonas campestris* pv. *campestris*
Xcci	*Xanthomonas citri* subsp. *citri*
Xoc	*Xanthomonas oryzae* pv. *oryzicola*
Xoo	*Xanthomonas oryzae* pv. *oryzae*
Xrv	*Xanthomonas* regulator of virulence

Supplementary Information

The online version contains supplementary material available at https://doi.org/10.1186/s42483-023-00197-7.

Additional file 1: Figure S1. Comparison of the predicted amino acid sequences of XrvA, XrvB, and XrvC in *Xoc* strain GX01. **Figure S2**. The XrvA and XrvC in *Xoc* do not impact HR induction on nonhost plant. **Figure S3**. XrvA and XrvC do not bind the *hrpG* promoter region. **Figure S4**. The level of EPS and extracellular enzymes produced by the *xrvB* deletion mutant was similar to that of the wild type in *Xoc*.

Additional file 2: Table S1. Bacterial strains and plasmids used in this work. **Table S2**. Primers used in this study.

Acknowledgements

Not applicable.

Author contributions

GL and RL conceived and designed the project. JP, JS, WY, and QS carried out the experiments. ZM, XZ, GZ, and JT provided the resources and analyzed the data. GL, RL, JP, and JS wrote the manuscript.

Funding

This work was supported by the National Natural Science Foundation of China (32160617; 32260501).

Availability of data and materials

The data that support the findings of this study are available from the corresponding author upon reasonable request.

Declarations

Ethics approval and consent to participate

Not applicable.

Consent for publication

Not applicable.

Competing interests

The authors declare that they have no competing interests.

Received: 25 May 2023 Accepted: 19 August 2023
Published online: 11 September 2023

References

An SQ, Lu GT, Su HZ, Li RF, He YQ, Jiang BL, et al. Systematic mutagenesis of all predicted *gntR* genes in *Xanthomonas campestris* pv. *campestris* reveals a GntR family transcriptional regulator controlling hypersensitive response and virulence. Mol Plant Microbe Interact. 2011;24(9):1027–39. https://doi.org/10.1094/MPMI-08-10-0180.

An SQ, Potnis N, Dow M, Vorhölter FJ, He YQ, Becker A, et al. Mechanistic insights into host adaptation, virulence and epidemiology of the phytopathogen *Xanthomonas*. FEMS Microbiol Rev. 2020;44(1):1–32. https://doi.org/10.1093/femsre/fuz024.

Andrade MO, Farah CS, Wang N. The post-transcriptional regulator *rsmA/csrA* activates T3SS by stabilizing the 5′UTR of *hrpG*, the master regulator of *hrp/hrc* genes, in *Xanthomonas*. PLoS Pathog. 2014;10(2):e1003945. https://doi.org/10.1371/journal.ppat.1003945.

Bertin P, Hommais F, Krin E, Soutourina O, Tendeng C, Derzelle S, Danchin A. H-NS and H-NS-like proteins in Gram-negative bacteria and their multiple role in the regulation of bacterial metabolism. Biochimie. 2001;83(2):235–41. https://doi.org/10.1016/s0300-9084(01)01247-0.

Büttner D, Bonas U. Regulation and secretion of *Xanthomonas* virulence factors. FEMS Microbiol Rev. 2010;34(2):107–33. https://doi.org/10.1111/j.1574-6976.2009.00192.x.

Cui P, Li RF, Zhang DP, Tang JL, Lu GT. HpaP, a novel regulatory protein with ATPase and phosphatase activity, contributes to full virulence in *Xanthomonas campestris* pv. *campestris*. Environ Microbiol. 2018;20(4):1389–404. https://doi.org/10.1111/1462-2920.14046.

Dorman CJ. H-NS: a universal regulator for a dynamic genome. Nat Rev Microbiol. 2004;2(5):391–400. https://doi.org/10.1038/nrmicro883.

Feng JX, Song ZZ, Duan CJ, Zhao S, Wu YQ, Wang C, et al. The *xrvA* gene of *Xanthomonas oryzae* pv. *oryzae*, encoding an H-NS-like protein, regulates virulence in rice. Microbiology. 2009;155(9):3033–44. https://doi.org/10.1099/mic.0.028910-0.

Kametani-Ikawa Y, Tsuge S, Furutani A, Ochiai H. An H-NS-like protein involved in the negative regulation of *hrp* genes in *Xanthomonas oryzae* pv. *oryzae*. FEMS Microbiol Lett. 2011;319(1):58–64. https://doi.org/10.1111/j.1574-6968.2011.02266.x.

Li RF, Lu GT, Li L, Su HZ, Feng GF, Chen Y, et al. Identification of a putative cognate sensor kinase for the two-component response regulator HrpG, a key regulator controlling the expression of the *hrp* genes in *Xanthomonas campestris* pv. *campestris*. Environ Microbiol. 2014;16(7):2053–71. https://doi.org/10.1111/1462-2920.12207.

Li L, Li RF, Ming ZH, Lu GT, Tang JL. Identification of a novel type III secretion-associated outer membrane-bound protein from *Xanthomonas campestris* pv. *campestris*. Sci Rep. 2017;7:42724. https://doi.org/10.1038/srep42724.

Li RF, Wang XX, Wu L, Huang L, Qin QJ, Yao JL, et al. *Xanthomonas campestris* sensor kinase HpaS co-opts the orphan response regulator VemR to form a branched two-component system that regulates motility. Mol Plant Pathol. 2020;21(3):360–75. https://doi.org/10.1111/mpp.12901.

Li RF, Ren PD, Liu QQ, Yao JL, Wu L, Zhu GN, et al. McvR, a single domain response regulator regulates motility and virulence in the plant pathogen *Xanthomonas campestris*. Mol Plant Pathol. 2022;23(5):649–63. https://doi.org/10.1111/mpp.13186.

Li RF, Ren PD, Zhang DP, Cui P, Zhu GN, Xian XY, et al. HpaP divergently regulates the expression of *hrp* genes in *Xanthomonas oryzae* pathovars *oryzae* and *oryzicola*. Mol Plant Pathol. 2023;24(1):44–58. https://doi.org/10.1111/mpp.13276.

Liao ZX, Ni Z, Wei XL, Chen L, Li JY, Yu YH, et al. Dual RNA-seq of *Xanthomonas oryzae* pv. *oryzicola* infecting rice reveals novel insights into bacterial-plant interaction. PLoS ONE. 2019;14(4):e0215039. https://doi.org/10.1371/journal.pone.0215039.

Liu Y, Long J, Shen D, Song C. *Xanthomonas oryzae* pv. *oryzae* requires H-NS-family protein XrvC to regulate virulence during rice infection. FEMS Microbiol Lett. 2016;363(10):fnw067. https://doi.org/10.1093/femsle/fnw067.

Liu GF, Su HZ, Sun HY, Lu GT, Tang JL. Competitive control of endoglucanase gene *engXCA* expression in the plant pathogen *Xanthomonas campestris* by the global transcriptional regulators HpaR1 and Clp. Mol Plant Pathol. 2019;20(1):51–68. https://doi.org/10.1111/mpp.12739.

Long JJ, Jahn CE, Sánchez-Hidalgo A, Wheat W, Jackson M, Gonzalez-Juarrero M, et al. Interactions of free-living amoebae with rice bacterial pathogens *Xanthomonas oryzae* pathovars *oryzae* and *oryzicola*. PLoS ONE. 2018;13(8):e0202941. https://doi.org/10.1371/journal.pone.0202941.

Mansfield J, Genin S, Magori S, Citovsky V, Sriariyanum M, Ronald P, et al. Top 10 plant pathogenic bacteria in molecular plant pathology. Mol Plant Pathol. 2012;13(6):614–29. https://doi.org/10.1111/j.1364-3703.2012.00804.x.

Müller CM, Schneider G, Dobrindt U, Emödy L, Hacker J, Uhlin BE. Differential effects and interactions of endogenous and horizontally acquired H-NS-like proteins in pathogenic *Escherichia coli*. Mol Microbiol. 2010;75(2):280–93. https://doi.org/10.1111/j.1365-2958.2009.06995.x.

Niño-Liu DO, Ronald PC, Bogdanove AJ. *Xanthomonas oryzae* pathovars: model pathogens of a model crop. Mol Plant Pathol. 2006;7(5):303–24. https://doi.org/10.1111/j.1364-3703.2006.00344.x.

Niu XN, Li Y, Carpenter S, Dan X, Li T, Wu Q, et al. Complete genome resource of *Xanthomonas oryzae* pv. *oryzicola* GX01 isolated in south China. Mol Plant Microbe Interact. 2022;35(4):357–9. https://doi.org/10.1094/MPMI-10-21-0259-A.

Qin L, Erkelens AM, Ben Bdira F, Dame RT. The architects of bacterial DNA bridges: a structurally and functionally conserved family of proteins. Open Biol. 2019;9(12):190223. https://doi.org/10.1098/rsob.190223.

Rashid MM, Ikawa Y, Tsuge S. GamR, the LysR-Type galactose metabolism regulator, regulates *hrp* gene expression via transcriptional activation of two key *hrp* regulators, HrpG and HrpX, in *Xanthomonas oryzae* pv. *oryzae*. Appl Environ Microbiol. 2016;82(13):3947–58. https://doi.org/10.1128/AEM.00513-16.

Sambrook J, Fritsch EF, Maniatis T. Molecular cloning: a laboratory manual. 2nd ed. New York: Cold Spring Harbor; 1989.

Schäfer A, Tauch A, Jäger W, Kalinowski J, Thierbach G, Pühler A. Small mobilizable multi-purpose cloning vectors derived from the *Escherichia coli* plasmids pK18 and pK19: selection of defined deletions in the chromosome of *Corynebacterium glutamicum*. Gene. 1994;145(1):69–73. https://doi.org/10.1016/0378-1119(94)90324-7.

Staskawicz B, Dahlbeck D, Keen N, Napoli C. Molecular characterization of cloned avirulence genes from race 0 and race 1 of *Pseudomonas syringae* pv. *glycinea*. J Bacteriol. 1987;169(12):5789–94. https://doi.org/10.1128/jb.169.12.5789-5794.1987.

Su HZ, Wu L, Qi YH, Liu GF, Lu GT, Tang JL. Characterization of the GntR family regulator HpaR1 of the crucifer black rot pathogen *Xanthomonas campestris* pathovar *campestris*. Sci Rep. 2016;6:19862. https://doi.org/10.1038/srep19862.

Sukchawalit R, Vattanaviboon P, Sallabhan R, Mongkolsuk S. Construction and characterization of regulated L-arabinose-inducible broad host range expression vectors in *Xanthomonas*. FEMS Microbiol Lett. 1999;181(2):217–23. https://doi.org/10.1111/j.1574-6968.1999.tb08847.x.

Tang JL, Liu YN, Barber CE, Dow JM, Wootton JC, Daniels MJ. Genetic and molecular analysis of a cluster of *rpf* genes involved in positive regulation of synthesis of extracellular enzymes and polysaccharide in *Xanthomonas campestris* pathovar *campestris*. Mol Gen Genet. 1991;226(3):409–17. https://doi.org/10.1007/BF00260653.

Tendeng C, Bertin PN. H-NS in Gram-negative bacteria: a family of multifaceted proteins. Trends Microbiol. 2003;11(11):511–8. https://doi.org/10.1016/j.tim.2003.09.005.

Teper D, Pandey SS, Wang N. The HrpG/HrpX regulon of xanthomonads-an insight to the complexity of regulation of virulence traits in phytopathogenic bacteria. Microorganisms. 2021;9(1):187. https://doi.org/10.3390/microorganisms9010187.

Tsuge S, Furutani A, Fukunaka R, Oku T, Tsuno K, Ochiai H, et al. Expression of *Xanthomonas oryzae* pv. *oryzae hrp* genes in XOM2, a novel synthetic medium. Gen Plant Pathol. 2002;68(4):363–71. https://doi.org/10.1007/PL00013104.

Turner P, Barber CE, Daniels MJ. Evidence for clustered pathogenicity genes in *Xanthomonas campestris* pv. *campestris*. Mol Gen Genet. 1985;199(2):338–43. https://doi.org/10.1007/BF00330277.

Wang H, Ayala JC, Silva AJ, Benitez JA. The histone-like nucleoid structuring protein (H-NS) is a repressor of *Vibrio cholerae* exopolysaccharide biosynthesis (*vps*) genes. Appl Environ Microbiol. 2012;78(7):2482–8. https://doi.org/10.1128/AEM.07629-11.

Zhang H, Wang S. Rice versus *Xanthomonas oryzae* pv. *oryzae*: a unique pathosystem. Opin Plant Biol. 2013;16(2):188–95. https://doi.org/10.1016/j.pbi.2013.02.008.

Zhang Y, Teper D, Xu J, Wang N. Stringent response regulators (p)ppGpp and DksA positively regulate virulence and host adaptation of *Xanthomonas citri*. Mol Plant Pathol. 2019;20(11):1550–65. https://doi.org/10.1111/mpp.12865.

Zhou X, Yan Q, Wang N. Deciphering the regulon of a GntR family regulator via transcriptome and ChIP-exo analyses and its contribution to virulence in *Xanthomonas citri*. Mol Plant Pathol. 2017;18(2):249–62. https://doi.org/10.1111/mpp.12397.

Zhou X, Teper D, Andrade MO, Zhang T, Chen S, Song WY, et al. A Phosphorylation switch on Lon protease regulates bacterial type III secretion system in host. Mbio. 2018;9(1):e02146-e2217. https://doi.org/10.1128/mBio.02146-17.

Zou LF, Wang XP, Xiang Y, Zhang B, Li YR, Xiao YL, et al. Elucidation of the *hrp* clusters of *Xanthomonas oryzae* pv. *oryzicola* that control the hypersensitive response in nonhost tobacco and pathogenicity in susceptible host rice. Appl Environ Microbiol. 2006;72(9):6212–24. https://doi.org/10.1128/AEM.00511-06.